NEUTRON-INDUCED CAVITATION TENSION METASTABLE PRESSURE THRESHOLDS OF LIQUID MIXTURES

Y. XU*, J. A. WEBSTER, J. LAPINSKAS and R. P. TALEYARKHAN
School of Nuclear Engineering, Purdue University, West Lafayette, IN 47907
*Corresponding author. E-mail : yiban@purdue.edu

Invited August 18, 2008
Received October 30, 2008

Tensioned metastable fluids provide a powerful means for low-cost, efficient detection of a wide range of nuclear particles with spectroscopic capabilities. Past work in this field has relied on one-component liquids. Pure liquids may provide very good detection capability in some aspects, such as low thresholds or large radiation interaction cross sections, but it is rare to find a liquid that is a perfect candidate on both counts. It was hypothesized that liquid mixtures could offer optimal benefits and present more options for advancement. However, not much is known about radiation-induced thermal-hydraulics involving destabilization of mixtures of tensioned metastable fluids. This paper presents results of experiments that assess key thermophysical properties of liquid mixtures governing fast neutron radiation-induced cavitation in liquid mixtures. Experiments were conducted by placing liquid mixtures of various proportions in tension metastable states using Purdue's centrifugally-tensioned metastable fluid detector (CTMFD) apparatus. Liquids chosen for this study covered a good representation of both thermal and fast neutron interaction cross sections, a range of cavitation onset thresholds and a range of thermophysical properties. Experiments were devised to measure the effective liquid mixture viscosity and surface tension. Neutron-induced tension metastability thresholds were found to vary non-linearly with mixture concentration; these thresholds varied linearly with surface tension and inversely with mixture vapor pressure (on a semi-log scale), and no visible trend with mixture viscosity nor with latent heat of vaporization.

KEYWORDS : Neutron-Induced Cavitation, Tensioned Metastable Pressure Threshold, Liquid Mixtures

1. INTRODUCTION

Radiation-induced cavitation or nucleation for liquids in metastable states allows one to utilize this phenomenon for nuclear particle detection. Indeed, Glaser (1958) received the *Nobel Prize* for his work on the bubble chamber wherein bubbles are formed in a thermally superheated liquid when nuclear particles strike the metastable fluid. This realization has resulted in the development of so-called superheated droplet detectors (SDDs) (Apfel, 1979, Ing, 1997). However, SDDs require the fluid-state to be thermally-superheated and the intrinsic efficiency for detection from such systems inherently suffers due to the need for spatial separation of superheated droplets in host liquids by factors of ~ 1,000. A more interesting and useful means for detection of radiation that we have studied and developed (Lapinskas et al. (2006); Smagacz et al. (2006); Xu et al. (2006); Taleyarkhan et al. (2006)) relies on liquids in "tensioned" metastable states allowing room temperature operation. In such a system the entire tensioned volume is sensitive. Therefore, such a system will have intrinsic efficiencies higher than those of SDDs by a factor of ~ 1,000.

It has been known, although not widely appreciated, for some time, that liquids, like solids, can indeed be put under negative pressure (below perfect vacuum). Although surprising at first, this was confirmed via elegant experiments reported in *Science* (Scholander et al., 1965). Since Glaser's discovery, sporadic efforts were also attempted to examine radiation-induced cavitation in tensioned liquids (Greenspan et al., 1967; Lieberman, 1958). These earlier efforts employed large, complex and/or expensive apparatus. More recently, this technique was successfully employed for attaining supercompression and thermonuclear fusion states in deuterated liquids (Forringer et al., 2006; Taleyarkhan et al., 2002, 2004, 2006; Lahey et al., 2005; Nigmatulin et al., 2005; Xu et al, 2005).

Radiation-induced cavitation or nucleation involves several distinctive physical phenomena including radiation type, linear-energy transfer rate, probability of interaction on nuclear and atomic scales, physical properties of the target molecules, etc. A given liquid has unique properties that are useful in detection. However, this may not necessarily attain all of the desired characteristics (e.g., volatility, safety, sensitivity, etc.). All known past studies have been conducted with single molecule liquids. Studies with mixtures of molecules could offer a huge leap in possible combination of key parameters determining the

applicability for certain field conditions and is the subject of this manuscript.

The nucleation of bubbles in liquids can be reasonably-well understood via kinetic theory (Fisher, 1948). For a nucleated bubble to grow rather than collapse requires that the size exceed a certain critical radius, r_c, given by,

$$r_c = \frac{2\sigma}{P_v - P_l}, \tag{1}$$

where σ is the liquid surface tension, P_v and P_l are vapor pressure and liquid pressure, respectively. Seitz's thermal-spike theory (Seitz, 1968) developed for bubble chambers captures essential energy components required for the incoming radiation particle to allow growth of the nucleated bubble to the critical radius and can be written as

$$E_c = \frac{4\pi}{3} r_c^3 \rho_v h_{fg} + 4\pi r_c^2 \left(\sigma - T\frac{\partial\sigma}{\partial T}\right) + \frac{4\pi}{3} r_c^3 P_l + W_k + W_J + W_{visc} + W_h \tag{2}$$

The first three terms of eq. (2) are the thermodynamically reversible processes of vaporization, formation of void surface, and bubble expansion against liquid pressure. The next four (irreversible) terms account for kinetic energy (W_k), acoustic radiation (W_J), viscosity dissipation (W_{visc}) and conductive heat loss (W_h), which are minor contributors for water and most of organic liquids (Bell et. al, 1974). Note that P_l is the ambient pressure in liquids and it has negative values in this study. Therefore, in eq. (2), the negative pressure provides the energy supply for the void growth and this is similar to the superheating of liquids in SDDs. Also, since P_l in eq. (1) is negative, the required values of r_c are much smaller for tensioned metastable liquids versus those in the thermally-superheated states.

From eq. (2) we see that the liquid properties of surface tension, vapor pressure, latent heat of vaporization and viscosity will play important roles in radiation-induced detection. While these have to be convoluted with the impact of nuclear-scale cross-sections of interaction with incoming nuclear particles, nevertheless, it was considered important to assess neutron detection in tension states in conjunction with key fluid (single and multi-component) mixtures.

This paper is focused on presentation of experimental results for neutron-induced cavitation of fluid mixtures and the variation of thresholds with physical properties.

2. EXPERIMENTAL APPARATUS AND DATA REDUCTION

Tensioned metastable states in fluid mixtures can be attained using various apparatus and types and approaches that we have described elsewhere (Smagacz et al., 2006; Lapinskas et al., 2006; Xu et al., 2006). The present studies were conducted using a centrifugal tensioned metastable fluid detector (CTMFD) based apparatus (Xu, et.al, 2006). Figure 1 shows a schematic of the experimental apparatus. In such an apparatus, the tension (negative) pressure (Pn) distribution for the liquid in the two side-arms is built up from the centerline bulb region and can be expressed as

$$P_n(r) = 2\pi^2 \rho_l f^2 \left(R^2 - r^2\right) - P_{amb} \tag{3}$$

where r is the radius from the center line, R (around 15 cm) is the radius of the liquid meniscus between the liquid interface and centerline, P_{amb} is the ambient pressure in the gas space, and f is the rotating frequency. Apparently, the maximum negative pressure in the detector is located at the center line of the center bulb when r=0. The servo motor was controlled by a LabView™-based computer program with user-defined rotating frequency, waiting time for detection before ramp down/up, delay time between consecutive operations, and ramp rate. The system is stopped by the control program manually by the operator

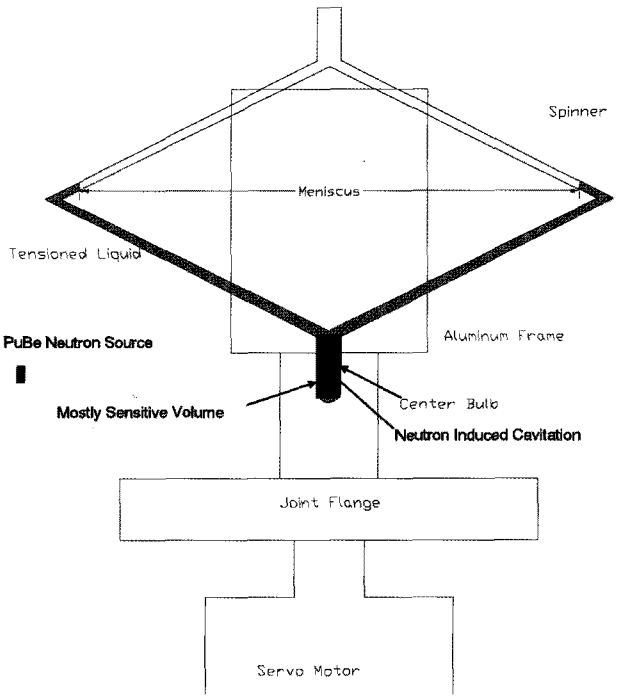

Fig. 1. Schematic of Experimental Apparatus

when an audible signal is noted from a detected nucleation event. Therefore, the least-count for onset of a detection event is uncertain to a few seconds (typically < 3 s).

Each test run started with the CTMFD initially at rest. In order to reduce the uncertainty in experimental results, several runs for a given rotating frequency were repeated with the same preset values of ramp rate, waiting time for detection, and delay time between consecutive operations. The waiting time for an event to occur was constrained by the need to protect the motor from overheating and the delay time was necessary for the bubble releasing to the liquid and gas interface. The liquid meniscus in the detector was measured before and after individual experiments to make sure that it did not change significantly during the experiment. For each experiment, control runs were always conducted without the presence of a neutron source. A sufficiently high rotation frequency, defined herein as upper limit rotating frequency (ULRF), was first ensured without spurious count occurrence to reduce the probability of false positives. Thereafter, neutron detection experimental runs were conducted at lower rotating frequencies than the ULRF. A 1 Ci PuBe neutron source (a cylindrical shape with 2.54 cm outside diameter and 4 cm height) was fixed at the same location for all of the tests, excluding the neutron flux and spectrum effects from the testing results. It was observed that initial degassing was necessary so that the CTMFD could reach the required negative pressures without cavitation in the absence of neutron sources. There is no need to ensure complete absence of gas and/or impurities in liquids if spontaneous cavitation thresholds are substantially larger (i.e., 2 times or more) than corresponding liquids with neutron induced cavitation.

The experimental errors were estimated as follows: the rotating frequency fluctuated within 0.05 Hz of the given value; the meniscus was measured with an uncertainty less than 0.2 cm; liquid density was calculated based on the room temperature which may be slightly different from the liquid in the device (i.e., <1% variation). Temperatures of liquid and rotating device were not measured directly each time; instead a thermocouple was installed in the air near the rotating device. From experience we have found that, for such experimental conditions, the glass temperature varied by only ~1 °C. Due to strong air flow driven by the rotating device, no significant temperature variation was observed during experimental runs. Furthermore, a Nylon joint was used between the motor and the detector to reduce heat conduction. Consequently, liquid temperature was not significantly different from room temperature (21 °C). The response time was determined with an uncertainty typically less than 3 s.

2.1 Test Matrix

Several commonly used liquids and their mixtures were used in this study. The mixtures were made using Eppendorf® pipettes (<1% volume variation) and their masses were measured when the two liquids were mixed together for quality control purposes. No chemical reaction related effects were observed during mixing since these chemicals have zero reactivity as also evidenced from information in their Material Safety Data Sheets. Table 1 lists a matrix of the samples used in this study. The concentrations listed are the volume ratios of the secondary fluids in the mixtures. The thermophysical properties of pure liquids are listed in Table 2, which were obtained from a chemical properties handbook (http://www.knovel.com/knovel2).

Table 1. Test Matrix of Liquid Mixtures in Volume Fractions of Secondary Liquids

Secondary Primary	Ethylene Glycol	Benzene	Tetrachloroethylene
Acetone	0.0, 0.125, 0.25, 0.375, 0.5, 0.625, 0.75	0.0, 0.25, 0.5, 0.75, 1.0	0.0, 0.25, 0.5, 0.75, 1.0
Benzene			0.0, 0.25, 0.5, 0.75, 1.0

Table 2. Thermophysical Properties of Pure Liquids at 21 °C

Properties at 21 °C	Threshold (bar)*	Vapor Pressure (kPa)	Surface Tension (mN/m)	Viscosity (mPas)	Latent Heat of Vaporization (kJ/mol)
Acetone	3.5	24.5	23.5	0.319	32.5
Benzene	12.5	10.0	28.7	0.644	34.7
Tetrachloroethylene	7	1.9	30.1	0.843	39.6
Ethylene Glycol	36	0.008	50.6	20.888	69.3

* Note: These values were obtained by authors when using the specific device, neutron source and operation conditions. The last one was extrapolated from the fitting curve.

2.2 Data Reduction

Neutron-induced cavitation was observed at several rotating speeds and several runs were repeated to improve accuracy. The response time ranged from a few seconds to 1 minute and a typical result is shown in Figure 2. Threshold pressure is defined as the negative pressure corresponding to detection of cavitation with the response time at about 10 s for the given neutron source at a fixed location. A pre-operation without a neutron source and without cavitation at sufficiently large negative pressures (normally twice of the thresholds) was done to ensure there was no spontaneous cavitation in radiation induced cavitation runs.

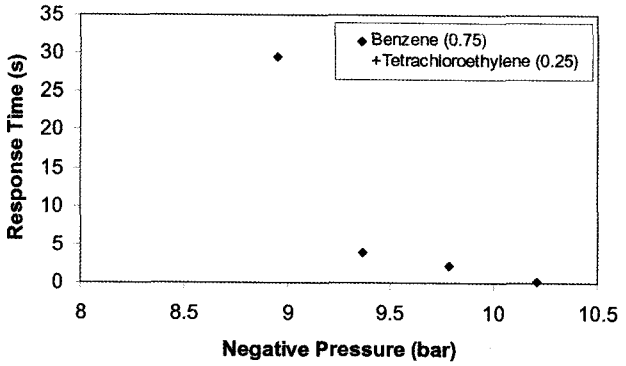

Fig. 2. A typical Result of Response Time vs. Negative Pressures

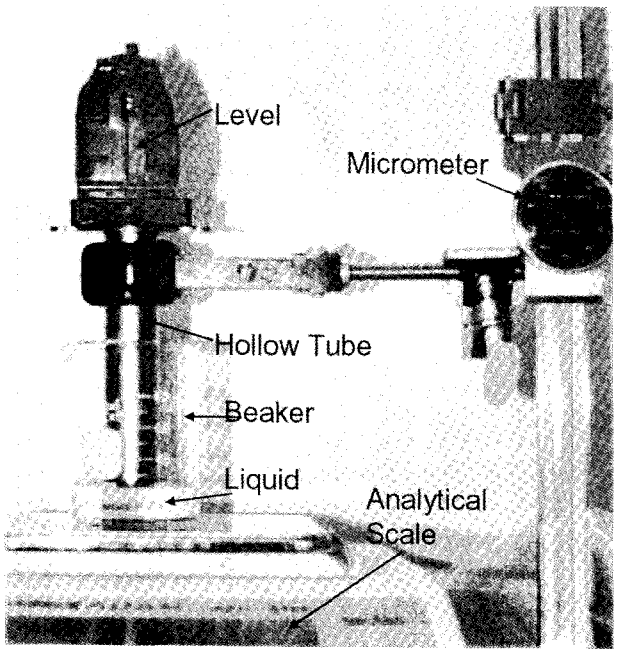

Fig. 3. Setup of Surface Tension Measurement

The response time of 10 s was chosen because of two reasons: (1) due to inherent, around ~3 s, measuring errors in the system, any response time shorter than 3 s shall have large system uncertainties; (2) it was clear that response time varies nonlinearly with the induced negative pressures. In general, 10 s was found to be a reasonable choice of distinction between higher and lower variations. The thresholds at 10 s were determined based on least square curve fitting.

It may be worthy to address statistics of the measured data. Radioactive decay itself is a random process, following a Poisson distribution for which one standard deviation error is readily obtained from the square roots of the mean values. The present data were obtained on average with 6 to 10 trials.

2.3 Thermophysical Properties of Liquid Mixtures – Estimation and Measurement

Thermophysical properties of liquid mixtures were estimated and/or measured. While some mixture properties can be readily calculated, it was not so for surface tension and viscosity of mixtures. This required the devising of separate experiments. Figure 3 illustrates the device used to measure surface tension of liquid mixtures. A liquid mixture was placed in a beaker set on an analytical scale with digital readout. A steel tube (coated with titanium) was submerged in the sample gradually. When the tube contacts with the liquid surface, part of the liquid rises on the tube inside and outside surfaces due to the action of surface tension. The tube then was moved up slowly by adjusting the micrometer until the reading of the scale reached a maximum negative value (indicative of the maximum pulling force). Note that after the liquid film between the tube and the liquid surface was broken up, some of the liquid was left on the tube surface. Vaporization is another factor of uncertainty, which is a strong function of liquid vapor pressure. Several attempts (3-5 times) were made for each mixture to reduce uncertainties and ensure repeatability.

The surface tension forces were measured directly from the forces acting on the tube divided by the wetting perimeters as illustrated in the following equation.

$$\sigma = \frac{F_{max} - F_{left}}{L\cos\theta} \tag{4}$$

When F_{max} is the maximum stretching force reached, the contact angle, θ, becomes zero in eq. (4). L is the wetting perimeter and F_{left} is the liquid weight left on the contact surface of the tube. Before employing this technique for liquid mixtures, it was first used to benchmark against published values for single component (pure) liquids to ensure that the approach will lead to reasonable predictions when applied to mixtures. Figure 4 indicates a comparison

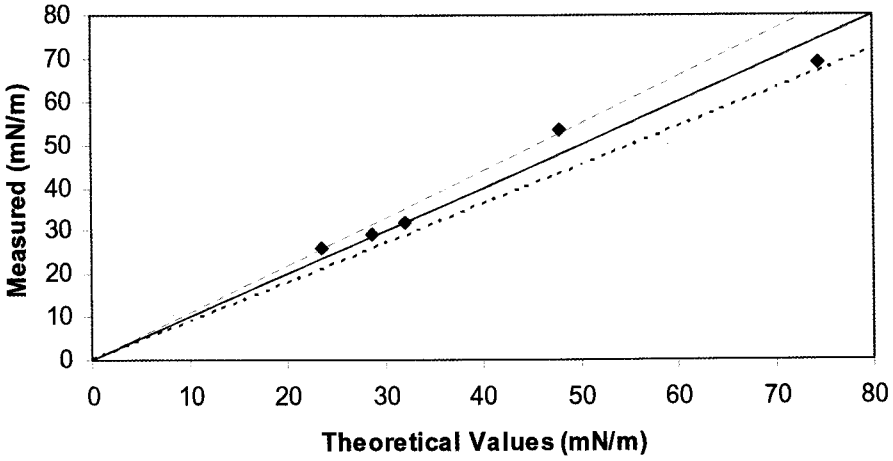

Fig. 4. Measured vs. Published Values of Surface Tension Forces for Pure Liquids

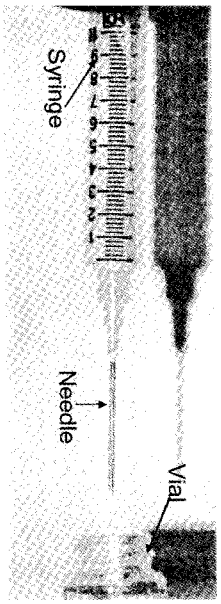

Fig. 5. Setup of Viscosity Measurement

between the measured values and published values of the pure liquids, which serves as a calibration check. It shows that the method has accuracy within +/-10% of the range of surface tension forces as shown with the dashed lines.

The viscosity of liquids was measured indirectly based on the establishment of laminar flow in a capillary tube (Digilov, 2005), for which the apparatus is shown in Figure 5. The upper part was a 10 cc plastic syringe providing a reservoir of liquid and the capillary tube was an 18G1-1/2 needle. A glass tube larger in diameter than the needle was used for liquid mixtures of high concentrations of ethylene glycol in acetone. The transient volume change of fluid in the syringe was recorded by a high speed digital video camera and a relation of liquid volume and time (t) was obtained from these images in a frame-by-frame fashion. A characteristic time, τ, (see eq. (5)) was obtained by fitting the curves of the measured volume and the calculated volume based on eq. (6).

$$\tau = \frac{8L_c S_t}{\pi r_c^4 \rho_l g}\mu \tag{5}$$

and

$$\alpha = \frac{\xi S_t}{\pi^2 r_c^4 g},\ \xi = 0.037\sqrt{\mathrm{Re}}, \xi = 1$$

was used in this calculation, which may introduce significant errors for large viscosities such as those of high concentrations of ethylene glycol. Fortunately, this was not the case as is shown by comparison against well-established correlations (Figure 6).

$$t = \tau\left\{\sqrt{1+\frac{4\alpha}{\tau^2}V_0} - \sqrt{1+\frac{4\alpha}{\tau^2}V} + \ln\left(\frac{\sqrt{1+\frac{4\alpha}{\tau^2}V_0}-1}{\sqrt{1+\frac{4\alpha}{\tau^2}V}-1}\right)\right\} \tag{6}$$

To ensure the quality of measured values, comparisons were made between the measured values and predicted values from Kendall's (Kendall and Monroe, 1917) additivity model and Mcallster's three body model (McAllster, 1964). It is clear that both models give reasonable predictions for the mixtures of acetone and ethylene glycol (see Figure 6(a)); however, it seems that McAllster's model works better at lower concentrations of tetrachloroethylene

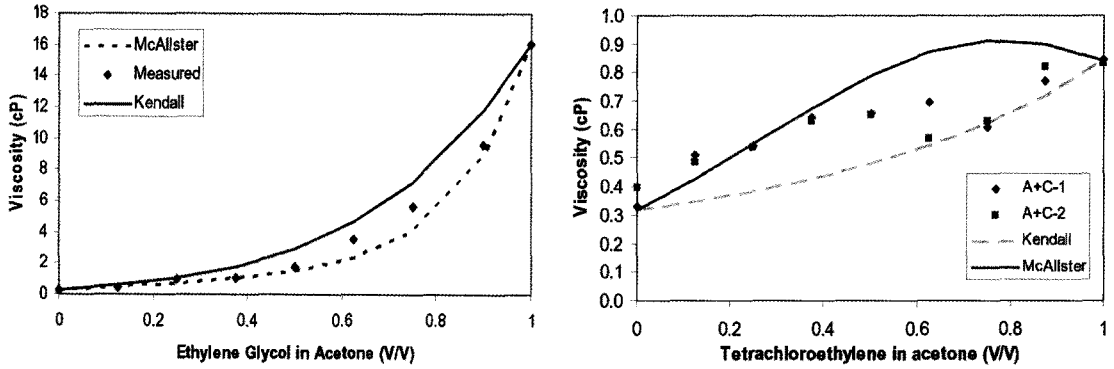

(a) acetone and ethylene glycol (b) acetone and tetrachloroethylene

Fig. 6. Comparison of Measured and Predicted Viscosities of Liquid Mixtures

in acetone while Kendall's model works favorably for high concentrations of the same mixtures (see Figure 6(b)). Note that the variation of viscosity in acetone and tetrachloroethylene is only twice while it is about 50 times in acetone and ethylene glycol mixtures. The latter may indicate the mixture viscosity is dominated by that of ethylene glycol. Nevertheless, the results concluded that the measurement approach is acceptable for the current analysis even though the uncertainties may be large under some circumstances.

Vapor pressure for liquid mixtures P_v was estimated using the well-known Rauolt's law for two component liquid mixtures of fractional component, X_1, each with it's own vapor pressures P_{v1} and P_{v2}, and written as,

$$P_v = X_1 P_{v1} + (1 - X_1) P_{v2}. \quad (7)$$

Theoretical prediction of latent heat of vaporization is neither simple, nor accurate. Many models (such as Santrach and Lielmezs, 1978; Akasaka, et. al, 2005) have been proposed to correlate the known thermodynamic properties and properties of the mixtures to predict the heat of vaporization of binary or multicomponent mixtures. Unfortunately, some of them were tedious to apply and others may be impractical. The correlation proposed by Tamir (1983) for multicomponent mixtures as a function of temperature and acentric factor (ω) is relatively easy to use, but it was difficult to verify its accuracy for the tested mixtures in this study.

$$h_{fg} = 8.345\times10^{-3} T_c(K) \left[\begin{array}{l} \left(11.944 - 11.476 T_r + 11.459 T_r^7\right) \\ +\omega\left(-1.9778 + 15.456 T_r - 21.057 T_r^7\right) \end{array} \right] \quad (8)$$

where,

$$\omega = \sum_{i=1}^{n} X_i \omega_i, \quad T_c = \sum_{i=1}^{n} \phi_i T_{ci}, \quad \phi_i = \frac{X_i V_{ci}^l}{\sum_{i=1}^{n} X_i V_{ci}^l}, \quad T_r = \frac{T}{T_c}.$$

3. PRELIMINARY RESULTS AND ANALYSES

3.1 Thresholds vs. Liquid Volume Fractions

A series of tests were conducted to observe the cavitation thresholds under the same neutron flux and spectrum emitted from a 1 Ci PuBe isotope neutron source (emitting ~ 2×10^6 n/s). The tension threshold was defined as the negative pressure (calculated from eq. (3)) at which the detector responded to the neutrons within ~10 s. The results of the experiments are summarized in Figure 7. Also shown are the least square curve fits of second order polynomial functions. It is clear that all of the results were sufficiently represented with the second order polynomials. The R^2 values are listed in Table 3 for a comparison purpose. Note that the highest mixture fraction of ethylene glycol was 0.75 because of limitations of the device for reaching larger negative pressures and difficulties of degassing the liquids. Liquid temperature was estimated as 21 °C (room temperature) and varied little (±0.5 °C) during the course of experimentation.

3.2 Thresholds vs. Liquid Mixture Properties

Figure 8 depicts the relationship between thresholds and liquid mixture properties. As pointed out previously, neutron-induced cavitation in metastable liquids involves several distinctive physical mechanisms including neutron flux and spectrum, neutron interaction cross section of materials, linear energy transfer of ions, and bubble nucleation in the liquid. The focus of this section is on

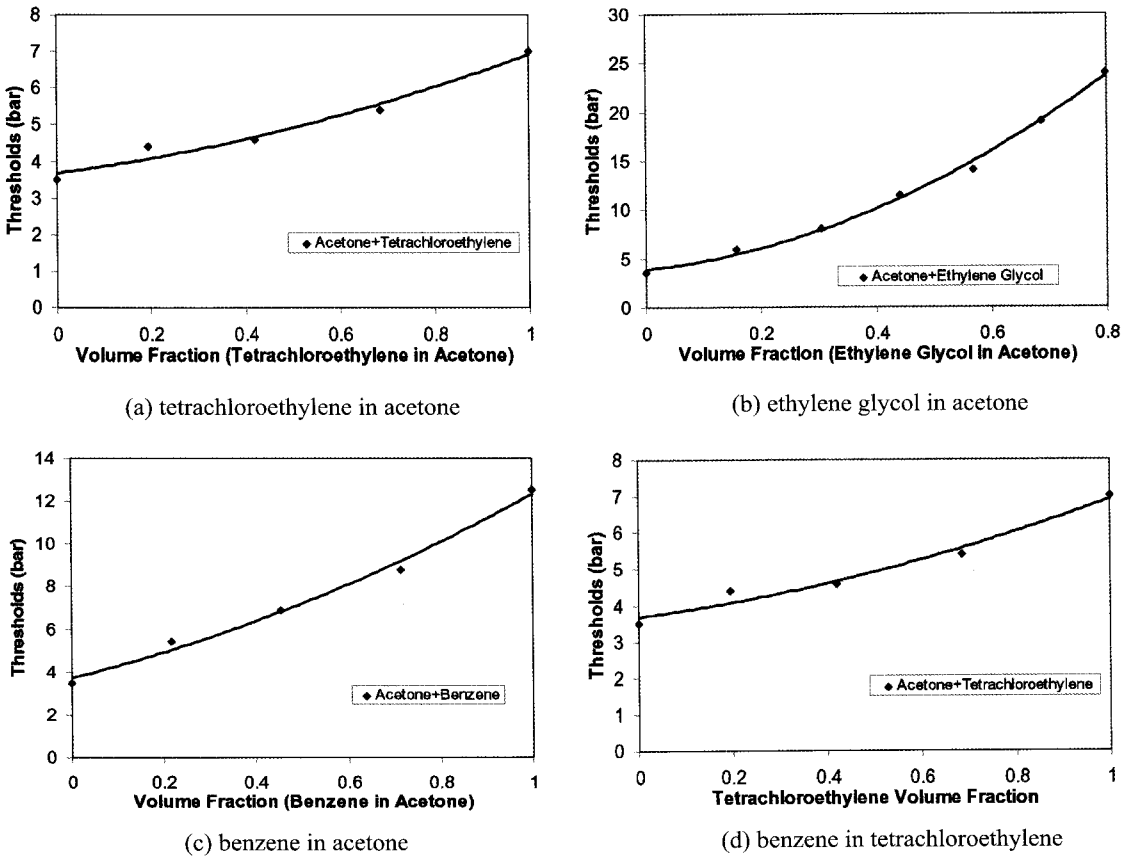

(a) tetrachloroethylene in acetone

(b) ethylene glycol in acetone

(c) benzene in acetone

(d) benzene in tetrachloroethylene

Fig. 7. Cavitation Thresholds vs. Volume Fractions of Liquid Mixtures

Table 3. R^2 Values (Quality of Curve Fittings)

	Linear	Second Order
Acetone + Ethylene Glycol	0.9732	0.9972
Acetone + Benzene	0.9656	0.9897
Acetone + Tetrachloroethylene	0.9238	0.9560
Tetrachloroethylene + Benzene	0.9131	0.9565

the thresholds variations with liquid properties under the conditions of a fixed neutron source and limited variations of the cross sections and linear energy transfers.

Mixtures of acetone and ethylene glycol and acetone and benzene have the same elements: C, H, and O. Therefore, it is reasonable to assume that these two mixtures will offer similar LETs and interaction cross sections for neutrons. It would be reasonable to assume that their thresholds differences are mainly governed by differing liquid properties. Among these four main contributors, the relations due to surface tensions and logarithmic vapor pressures are almost linear with almost the same slopes. This is in line with expectations for formation of critical radii, rc, as evidenced from the dependence of this key parameter in eq. (1).

It shall be noticed that the thresholds of the mixtures of acetone and tetrachloroethylene also follow a linear relation of surface tensions and logarithmic vapor pressures, but with a different (smaller) slope. This clearly indicates the interactions of neutrons with an additional element, Cl.

The case of mixtures of benzene and tetrachloroethylene is special and interesting because the two liquids have very similar thermophysical properties as seen in Table 2. Without considering the differences of nuclear interactions, one would believe that benzene should have lower thresholds since it has a higher vapor pressure, a lower surface tension and a smaller latent heat of vaporization. However, the experimental results indicate that the radiation induced cavitation threshold of benzene is higher than that of tetrachloroethylene for the same neutron source at the same distance. This strongly suggests that neutron cross section and linear energy transfer will play major and influential roles in detection and especially so for chlorine

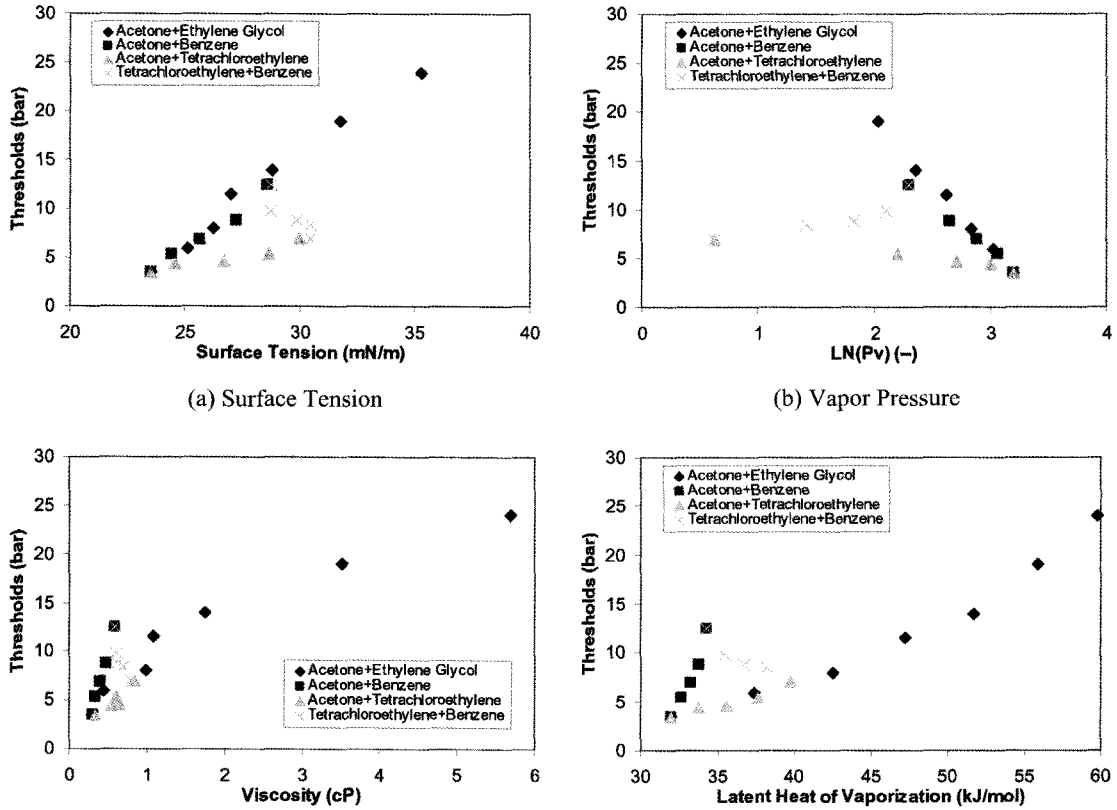

(a) Surface Tension

(b) Vapor Pressure

(c) Viscosity

(d) Latent Heat of Vaporization

Fig. 8. Cavitation Thresholds vs. Thermophysical Properties

atoms, which exhibit resonance peaks in the 0.1 to 0.5 MeV range and possess a relatively high (n, p) cross section at thermal neutron energies.

There does not appear to be a common consistency of trends of tension thresholds to viscosity as shown in Figure 8 (c), which indicates that viscosity may play a minor role for these selected liquid mixtures. However, it shall be pointed out that the other mixing pairs aside from acetone and ethylene glycol have very small variations of viscosity and as such a generalization is difficult to make at this stage. The same conclusion made for viscosity may also be applicable to dependence of tension thresholds on the latent heat of vaporization (see Figure 8 (d)).

A detailed quantitative analysis that includes considerations of energy for nucleation, complex nuclear interactions and multi-dimensional effects is beyond the scope of this paper.

4. SUMMARY AND CONCLUSION

In this study, we have conducted measurements of radiation-induced cavitation thresholds in various liquid mixtures. A quadratic dependence of tension threshold (from lowest to highest) was noted with mixture fractions. Good correlation of the mixture tension threshold was noted with surface tension and vapor pressure of the mixtures but not with the mixture viscosity, nor the latent heat of vaporization. It is yet unclear how precisely vapor pressure and surface tension play their respective roles in this process since the test matrix included the fluids with a limited range of surface tension forces. Nuclear interactions are expected to play a significant role in some liquid mixtures in which the physical property variations are small but when the elemental compositions are different. An integral, multi-dimensional thermal hydraulic-cum-nuclear particle transport based modeling-analyses effort is required to accommodate physical phenomena related to bubble nucleation with nuclear scale interactions of individual elements of mixture components.

ACKNOWLEDGEMENTS

The reported research was funded in part by Purdue Research Foundation and the State of Indiana (Purdue University). Past helpful discussions with Dr. Collin West are acknowledged.

NOMENCLATURE

BD	Bubble Detector
CTMFD	Centrifugal Tensioned Metastable Fluid Detector
E_c	Minimum Critical Energy of Nucleation
LET	Linear Energy Transfer
g	Gravitational Acceleration
h_{fg}	Latent Heat of Vaporization
L_c	Capillary Tube Length
n	Number of observations of cavitation
p	Probability of neutron interaction
P_{amb}	Ambient Pressure
P_l	Liquid Pressure
P_n	Negative Pressure in Liquid
P_v	Vapor Pressure
r_c	Capillary Tube Radius
R_c	Critical Void Radius
Re	Reynolds Number
S_t	Syringe Cross Section Area
SDD	Superheated Droplet Detectors
t	Time
T	Temperature
T_c	Liquid Critical Temperature
ULRF	Upper Limit Rotating Frequency
V	Liquid Volume in Syringe
V_0	Initial Liquid Volume in Syringe
V_{ci}	Liquid Critical Volume
W_h	Heat Loss due to Conduction
W_J	Work to Produce Acoustic Emission
W_{visc}	Energy Loss due to Viscosity Dissipation
W_k	Work Done to Produce Kinetic Energy
X_1	Mole Fraction of Component 1
X_2	Mole Fraction of Component 2, $X_1+X_2=1$ for binary mixtures

Symbols

α	Constant
ϕ	Variable Defined for eq. (8)
μ	Viscosity
ρ_v	Vapor Density
ρ_l	Liquid Density
τ	Characteristic Time Defined by eq. (5)
ω	Acentric Factor
ξ	Coefficient

REFERENCES

[1] R. Akasaka, T. Yamaguchi, T. Ito, "Practical and direct expressions of the heat of vaporization for mixtures", Chemical Engineering Science, 60, pp. 4369-4376, 2005.

[2] R. E., Apfel, "The superheated drop detector," *Nuclear Instruments and Methods*, Vol.162, Issues 1-3, pp. 603-608, June (1979).

[3] C. R. Bell, N. P. Oberle, W. Rohsenow, N. Todreas, and C. Tso, "Radiation-Induced Boiling in Superheated Water and Organic Liquids," *Nuclear Science and Engineering*, Vol.53, pp. 458-465, (1974).

[4] *Chemical properties handbook*, online at http://www.knovel.com/knovel2.

[5] R. M. Digilov, M. Reiner, "Weight-controlled capillary viscometer", *AM. J. Phys.*, Vol. 73, No. 11, pp. 1020-1022, Nov. (2005).

[6] E. Forringer, D. Robbins, J. Martin, "Confirmation of Neutron Production During Self-Nucleated Acoustic Cavitation", *Proc. Amer. Nucl. Soc.*, 736-737, Nov., (2006).

[7] D. A. Glaser, "The bubble chamber," *Encyclopedia of Physics*, 316-341, Nuclear Instrumentation II. S. Fluggeld, Springer-Verlag, (1958)

[8] M. Greenspan, C. E. Tschiegg, "Radiation-induced acoustic cavitation; threshold versus temperature for some liquids", *J. Acoustic Soc. Am.*, Vol.74, no.4, pp.1327-1331, Oct., (1982).

[9] B. Hahn, "The fracture of liquids under stress due to ionizing particles", *Nuovo Cimento*, Vol. 22, pp. 650-653, (1961).

[10] H. Ing, R. A. Noulty, and T. D. McLean, "Bubble detectors-A maturing technology", *Radiation Measurements*, Vol. 27, Issue 1, pp. 1-11, Feb. (1997).

[11] J. Kendall and K.P. Monroe, "The Viscosity of Liquids. II. The Viscosity-Composition Curve for Ideal Liquid Mixtures", J. Am. Chem. Soc. Vol. 39, No. 9, pp. 1787-1806, 1917.

[12] R. T. Lahey, R. P. Taleyarkhan, R. I. Nigmatulin and I. Akhatov, "Sonoluminescence and the search for Sonofusion", *Adv. in Heat Transfer*, Vol. 39, (2006).

[13] J. Lapinskas, P. Smagacz, J. Webster, P. Shaw, Y. Xu and R. P. Taleyarkhan, "Fast Neutron Gamma-Insensitive Continuous Operation Tension Metastable Fluid Detector," *Transac. Proc. Amer. Nucl. Soc. Conf.*, Reno, NV, (2006).

[14] D. Lieberman, "Radiation-induced cavitation", *The Physics of Fluids*, Vol.2, No.4, pp. 466-468, July-Aug., (1959).

[15] R. A. McAllster, "The Viscosity of Liquid Mixtures," *AIChE Journal*, Vol.6, No.3, pp. 427-431, (1959).

[16] R. I. Nigmatulin, I. Akhatov, A. Topolinokov, R. Bolotnova, N. Vakhitova, R. T. Lahey, Jr. and R. P. Taleyarkhan, "Theory of supercompression of vapor bubbles and nanoscale thermonuclear fusion", *Phys. of Fluids*, Vol.17, 107106, (2005).

[17] D. Santrach and J. Lielmezs, "The latent heat of vaporization prediction for binary mixtures", Industrial Engineering Chemical Fundamentals, Vol. 17, No. 2, pp. 93-96, 1978.

[18] F. Seitz, "On the theory of the bubble chamber," *The Physics of Fluids*, Vol.1, No.1, pp. 2-13, January-February, (1958).

[19] P. Smagacz, J. Lapinskas, A. Horn, Y. Xu and R. P. Taleyarkhan, "Fast Neutron Gamma-Insensitive Centrifugally-Tensioned Metastable Fluid Detector," *Transac. Proc. Amer. Nucl. Society*, Reno, NV, (2006).

[20] R. P. Taleyarkhan, C. D. West, J. Cho, R. T. Lahey, Jr., R. I. Nigmatulin and R. C. Block, "Evidence of nuclear emissions during acoustic cavitation," *Science*, Vol. 295, (2002).

[21] R. P. Taleyarkhan, J. Cho, C. D. West, R. T. Lahey, Jr., R. I. Nigmatulin and R. C. Block, "Additional Evidence of nuclear emissions during acoustic cavitation," *Phys. Rev. E.*, (2004).

[22] R. P. Taleyarkhan, C. D. West, R. T. Lahey, Jr., R. I. Nigmatulin, R. C. Block, and Y. Xu, "Nuclear emissions during self-nucleated acoustic cavitation," *Phys. Rev. Ltrs.*, (2006).

[23] A. Tamir, "Correlations for predicting azeotropic heat of vaporization of multicomponent mixtures," *Ind. Eng. Chem. Fundam.*, Vol.22, No.1, pp. 83-86, (1983).

[24] Y. Xu, and A. Butt, "Confirmation of nuclear emissions

during acoustic cavitation," *Nuclear Engineering and Design*, Vol. 235, pp. 1317-1324, (2005).
[25] Y. Xu, P. Smagacz, J. Lapinskas, J. Webster, P. Shaw and R. P. Taleyarkhan, "Neutron Detection with Centrifugally-Tensioned Metastable Fluid Detectors," *ICONE-14*, Miami, Florida, USA, July 17-20, (2006).